(DOI will not work until issue is live.) DOI: http://dx.doi.org/10.2138/am-2017-5857CCBYNCND

REVISION 2

Fluvial transport of impact evidence from cratonic interior to passive margin: Vredefort-derived shocked zircon on the Atlantic coast of South Africa

Stephanie D. Montalvo[a,b*], Aaron J. Cavosie[a,b,c], Timmons M. Erickson[a], and Cristina Talavera[d]

[a] Department of Applied Geology, Curtin University, Perth, Western Australia 6102, Australia

[b] Department of Geology, University of Puerto Rico, Mayagüez, PR 00681, USA

[c] NASA Astrobiology Institute, Department of Geoscience, University of Wisconsin-Madison, Madison, WI 53706 USA

[d] Department of Physics and Astronomy, Curtin University, Perth, Western Australia 6102, Australia

[*] Corresponding author Email address: s.montalvo@postgrad.curtin.edu.au

Abstract

Meteorite impacts produce shocked minerals in target rocks that record diagnostic high pressure deformation microstructures unique to hypervelocity processes. When impact craters erode, detrital shocked minerals can be transported by fluvial processes, as has been demonstrated through studies of modern alluvium at some of the largest known impact structures. In South Africa, detrital shocked minerals from the 2020 Ma Vredefort impact structure have been documented in the Vaal River basin, downriver from the structure. However, the ultimate fate of distally transported detrital shocked minerals in fluvial systems is not well understood, and is an important parameter for constraining the location of a source crater. Here, we report results of an extensive microstructural survey of detrital zircon from the Orange River basin and the Atlantic coast of South Africa to search for the presence of far-travelled Vredefort-derived detrital shocked zircon grains in different modern sedimentary environments. Three shocked grains were found out of 11,168 grains surveyed (0.03%) by scanning electron microscopy, including two in beach sand on the Atlantic coast and one from an Orange River sandbar 15 km upstream from the river mouth. Shock-produced {112} twins documented by electron backscatter diffraction in each of the three grains confirm their impact provenance, and U-Pb ages from 3130 to 3040 Ma are consistent with derivation from bedrock at the Vredefort impact structure. These results demonstrate the transport of Vredefort-derived shocked zircon to the coast via the Vaal-Orange river system, which requires 1940 km of fluvial transport from their point source on the Kaapvaal craton to the Atlantic coast passive margin. These results further demonstrate that shocked zircon grains can be detected in detrital populations at abundances < 1%, and can ultimately be transported outside their basin of origin when they arrive at continental margins. Detrital shocked zircon thus constitutes long-lived evidence of former impacts, as they retain microstructural evidence of shock deformation, as well as geochemical (U-Th-Pb) fingerprints of their source terrain. The study of detrital shocked minerals uniquely merges impact cratering with sedimentology, as identification of detrital grains with diagnostic shock microstructures in siliciclastic sediments can be applied to search the sedimentary record for evidence of eroded impact structures of any age, from the Phanerozoic to the Hadean, which can aid in reconstructing the impact record of Earth.

Keywords: shocked zircon; Vredefort impact structure; electron backscatter diffraction, Orange River; fluvial transport; shock metamorphism

Introduction

The terrestrial impact record has been largely removed due to geologic processes that obscure or destroy impact craters. Only 190 confirmed impact structures are currently recognized on Earth (Spray, 2001), while ~8700 impact structures >0.01 km in diameter have been identified on the Moon (Losiak et al., 2008). During meteorite impact, pressures and temperatures in target rocks can reach 100s of GPa and 1,000s of °C, greatly exceeding values of endogenic crustal metamorphism (Melosh, 1989). Under these conditions, certain minerals in target rocks record unique microstructures that form as a consequence of shock metamorphism (French, 1998; Leroux et al., 1999; Gibson and Reimold, 2008). Some shocked minerals eroded from impact structures, such as zircon, are resilient enough to survive as detrital grains. Identification of shock microstructures in detrital minerals can thus be used to detect evidence of impact structures that have been eroded or are otherwise unknown (Cavosie et al., 2010; Erickson et al., 2013a; Thomson et al., 2014; Reddy et al., 2015).

Shock features in zircon generally manifest as different types of planar microstructures that form from 20 to 40 GPa (Leroux et al., 1999) and include planar fractures (PFs), planar deformation features (PDFs), planar deformation bands (PDB), {112} twins, and the high pressure polymorph reidite (Wittmann et al., 2006; Timms et al., 2012; Erickson et al., 2013b; Cavosie et al., 2015a). Shocked zircon grains that experience high temperature can recrystallize to a granular texture consisting of neoblasts (Bohor et al., 1993; Cavosie et al., 2016), and ultimately dissociate. At present, {112} twins (Moser et al., 2011; Timms et al., 2012; Erickson et al., 2013a,b; Thomson et al., 2014; Cavosie et al., 2015b; Erickson et al., 2016) and the polymorph reidite (Glass and Liu, 2001; Wittmann et al., 2006; Cavosie et al., 2015a; Reddy et al., 2015) are considered the only diagnostic microstructural evidence for hypervelocity impact deformation of zircon.

Located southwest of Johannesburg in South Africa, the Vredefort Dome is a ~90 km wide erosional remnant that exposes the central uplift of one of the largest and oldest precisely dated impact structures on Earth (Fig. 1) (Wieland et al., 2005; Gibson and Reimold, 2008). It has been interpreted as a multi-ring structure originally ~300 km wide (Grieve and Therriault, 2000), and geothermobarometry studies of exposed rocks indicate that the upper 8 to 11 km have eroded since its formation at 2020 Ma (Kamo et al., 1996; Therriault et al., 1997; Gibson et al., 1998). Exposed components of the Vredefort impact structure include a ~40 km core of Archean granitoids and gneisses (Kamo et al., 1996; Hart et al., 1999; Moser et al., 2001; Flowers et al., 2003; Armstrong et al., 2006), surrounded by a ~20-25 km collar of late Archean to Paleoproterozoic metavolcanic and metasedimentary rocks (Wieland et al., 2005; Gibson and Reimold, 2008). Shocked zircon grains have been reported from a wide range of Vredefort bedrocks (e.g., Kamo et al., 1996; Gibson et al., 1997; Moser, 1997; Moser et al., 2011).

The Orange River is the largest river in South Africa, occupying a ~900,000 km^2 basin that drains roughly half of the Kaapvaal Craton (Fig. 1) (Bremner et al., 1990; Compton and Maake, 2007). The Vaal River is a right-bank tributary of the Orange River that flows through the Vredefort Dome in a generally southwest direction (Fig. 1). The combined Vaal-Orange fluvial system flows approximately 1940 km downstream from the Vredefort Dome to the Atlantic coast, where the Orange River has been discharging since the Cretaceous (de Wit et al., 2000; Gibbon et al., 2009; Garzanti et al., 2012). The location of the Orange River mouth has migrated between 31°S and its current location at 28°S over time (Dingle and Hendey, 1984). Currently, most Orange River discharge originates from the upper Orange, with < 2% contributed from below the Vaal-Orange confluence (Benade, 1988). At the outflow of the Orange River on the Atlantic Coast, longshore drift transport is from the south to the north, driven by the Benguela current (Fig. 1) (Garzanti et al., 2012). Once discharged, sediments from the Orange River are transported as far as the Namib Sand Sea on the Atlantic coast of Namibia by coastal and eolian processes (e.g., Garzanti et al., 2012).

Vredefort-derived detrital shocked minerals have previously been documented in the Vaal River, including zircon, monazite, and quartz, and are thus predicted to occur downstream in the Orange River. Cavosie et al. (2010) reported shocked zircon abundances of 36 – 64% in alluvium within the Vredefort Dome. Erickson et al. (2013a) documented detrital shocked zircon in the Vaal River outside the Vredefort Dome; at 103 km downstream from the impact structure, they found shocked zircon abundances of 18% in alluvium (81/452 grains). The most distal alluvium sample analyzed in that study was 759 km downstream from the impact structure, only ~3 km upriver from the Vaal-Orange confluence, which had a shocked zircon abundance of 2% (5/253 grains).

Given the ubiquitous occurrence of detrital shocked minerals in the Vaal River, the goal of this study is to evaluate if Vredefort-derived shocked zircon can be detected beyond the confluence of the Vaal and Orange rivers, at distal locations downstream from the Vredefort Dome in the Orange River. Samples of modern alluvium from the middle and lower Orange River, beach sand on the Atlantic coast of South Africa, and alluvium near the only other known impact structure in the Orange River basin were collected to test the extreme limits of distal transport, in terms of distance and detectability, for how far detrital shocked minerals can travel in a fluvial system, be identified, and linked to their source terrane. Given the time-intensive aspect of surveying large numbers of individual grains, our study focused exclusively on zircon.

Methodology

Fourteen sites were sampled to search for distally-transported detrital shocked zircon in modern sediment (Fig. 1, Table 1). These include seven alluvium samples from the middle and lower stretches of the Orange River below the Vaal-Orange confluence, and two heavy mineral beach sand samples at the Orange River mouth on the Atlantic coast. In addition to sampling Orange River alluvium and beach sand at the river mouth, five other sediment samples were collected to evaluate additional environments where detrital shocked zircon might reside. These include three samples of modern beach sand from south of the Orange River mouth, as far south as the mouth of the Oliphants River, to evaluate if shocked zircon grains are being transported northward along the Atlantic margin from previous locations where the Orange River discharged since the Cretaceous (Dingle and Hendey, 1984). Additionally, two modern alluvium samples near the Morokweng impact structure, the only other known impact structure in the Orange River basin, where collected to evaluate if detrital shocked zircon from this Jurassic-age structure are present in local fluvial systems that could potentially be transported by tributary streams to the Orange River.

Seven of the samples were collected in 2009 (09VDxx series), and seven in 2014 (14VDxx series); one of the 2009 sites on the Atlantic coast (09VD48) was resampled in 2014 (14VD80). Distances listed for samples in the Orange River are reported relative to the highway Route 53 bridge over the Vaal River at Parys, which is the closest point of the Vaal River to the center of the Vredefort impact structure. Distances listed for samples on the Atlantic coast and near the Morokweng impact structure are relative to the Orange River mouth. Samples were washed, dried and sieved to < 0.5 mm (1ϕ). Zircon grains were further concentrated using heavy liquids and a Frantz magnetic separator. Extreme care was taken to eliminate cross-sample contamination, as shocked zircon abundances were assumed to be low.

Zircon grains were handpicked and placed on aluminum scanning electron microscope (SEM) stubs. Documentation of shock microstructures on grain exteriors was done using backscattered electron imaging (BSE) with a Hitachi S-3400N SEM at the Eugene Cameron Electron Microprobe Lab at the University of Wisconsin-Madison. Further SEM analysis was conducted using a Tescan MIRA3 field emission gun (FEG) SEM at the Microscopy and Microanalysis Facility in the John de Laetre Centre at Curtin University. The FEG-SEM was used for BSE and panchromatic cathodoluminescence (CL) imaging, and electron backscatter diffraction (EBSD) analysis. Automated EBSD maps of regions of interest were generated by indexing electron backscatter diffraction patterns (EBSPs) on user-defined grids. Mean angular deviation values for each map ranged from 0.25 to 0.61°; the only post-collection filtering used was the wildspike correction. Maps of whole grains and smaller regions of interest were collected using step sizes ranging from 100 to 500 nm. EBSD analyses were collected with a 20 kV accelerating voltage, 70° sample tilt, 20.5 mm working distance, and 18 nA beam current. EBSPs were collected with a Nordlys Nano high resolution detector and Oxford Instruments Aztec system using routine data acquisition settings for zircon (e.g., Reddy et al., 2007). EBSD maps and pole figures were processed using the Tango and Mambo modules in the Oxford Instruments/HKL Channel 5 software package.

EBSD maps were used to illustrate different types of microstructures (figures 3, 4, 5). Band contrast (BC) maps display electron backscatter pattern quality, and were used as a background image to facilitate description of microstructures along with other EBSD maps. Texture component (TC) maps display variations in crystal orientation relative to a user-selected reference point (indicated by the red cross in figures 3c, 4c, 5c). Inverse pole figure (IPF) maps are color-coded according to Miller index to identify variations in crystallographic orientation. The grain boundary (GB) function inserts a colored line (red) along the boundary of adjacent pixels that form a specific misorientation about a specific axis. In figures 3, 4, and 5, the GB function was used to identify {112} twins, which are defined by a 65° misorientation about <110>.

U-Th-Pb geochronology data were collected for three shocked zircon grains. The grain from sample 09VD48 was analyzed using SHRIMP-RG in the SUMAC laboratory at Stanford University in 2010. Four analyses of grain 09VD48-2 were performed using a 25 μm primary beam. The $^{238}U/^{206}Pb$ ages obtained were calibrated with zircon standard R33 ($^{238}U/^{206}Pb$ age = 419 Ma) (Black et al., 2004), and U concentration was calibrated with zircon standard MAD (4196 ppm U) (Barth and Wooden, 2010). Grains from samples 14VD77 and 14VD80 were analyzed using SHRIMP II at Curtin University in 2015. SHRIMP II analyses were collected using a 20 μm diameter spot with a primary beam of 1.9 nA. A total of eight analyses were conducted on the two zircon grains, including five analyses of zircon 14VD80-373 and three analyses of zircon 14VD77-1224. The $^{238}U/^{206}Pb$ ages were calibrated with zircon standard R33, while U concentration was calibrated using zircon standard M257 (840 ppm U) (Nasdala et al., 2008). Data reduction was done using SQUID (Ludwig, 2001a) and ages calculated and plotted using Isoplot (Ludwig, 2001b).

Results

A total of 11,168 detrital zircon grains from the three disparate geographic areas of South Africa were surveyed to search for shock features. Shocked grains were only identified in three samples near the Orange River mouth on the Atlantic coast (Fig. 1b). A summary of the imaging and geochronological results is presented below.

Middle Orange River alluvium (5 sites, 2187 zircon grains)

From the middle Orange River a total of 2187 detrital zircon grains from five modern alluvium samples were surveyed. Samples 14VD69, 09VD38, 09VD44, 09VD45 and 09VD46

This is a preprint, the final version is subject to change, of the American Mineralogist (MSA)
Cite as Authors (Year) Title. American Mineralogist, in press.
(DOI will not work until issue is live.) DOI: http://dx.doi.org/10.2138/am-2017-5857CCBYNCND

represent alluvium at increasing distances of 761, 776, 1054, 1202, and 1219 km, respectively, downriver from the Vredefort Dome. Sample 14VD69 was collected from a sandbar 2 km downstream from the Vaal-Orange river confluence. No shocked zircon grains were found in the populations investigated, which ranged from 41 (09VD45) to 1153 (14VD69) grains per sample (Table 1).

Atlantic coast, near Orange River mouth (4 sites, 7326 zircon grains)

A total of 7326 zircon grains were surveyed from two modern alluvium samples collected from sandbars (14VD76, 14VD77), and two modern beach sand samples (09VD48, 14VD80) at and near the mouth of the Orange River, approximately 1940 km downriver from the Vredefort Dome. Three grains were identified that preserve conspicuous, closely-spaced (~5 µm) planar microstructures in multiple orientations on exterior surfaces (Fig. 2, Table 1). One of the grains was found in a sandbar 15 km upriver from the Atlantic coast (14VD77-1224) (Fig. 2a-c), and the other two grains were found in beach sand on the Atlantic coast at the mouth of the Orange River (09VD48-2 and 14VD80-373) (Fig. 2d-i). Each of the three sediment samples yielded a single detrital shocked zircon, which equates to abundances of 0.09% (1/1055, 09VD48), 0.04% (1/2745, 14VD80), and 0.03% (1/3174, 14VD77) per sample.

On polished surfaces, the PFs are readily visible with BSE and CL imaging. In zircon 14VD77-1224 three orientations of PFs, some of which offset the margin of the grain, are visible in the BSE image (Fig. 3a). Shock features are not obvious in the CL image of this grain, which shows both oscillatory and sector zoning (Fig. 3b). EBSD mapping revealed three sets of {112} shock-twins misoriented 65° <110> relative to the host grain, and <10° of cumulative misorientation across the grain accommodated by low-angle boundaries (Fig. 3c-e). Zircon 14VD80-373 shows one orientation of PFs in the BSE image (Fig. 4a). PFs are faintly visible in

CL (Fig. 4b), which shows a light rim around a dark core that appears disturbed. EBSD mapping revealed a set of {112} shock-twins in the same orientation as one of the PF sets (Fig. 4c-e). Up to 20° of cumulative misorientation across the grain was detected (Fig. 4c), however with the exception of grain margins, the majority of cumulative misorientation across the grain is <10°, and accommodated by low-angle boundaries. Zircon 09VD48-2 contains two sets of PFs visible in BSE and CL images (Fig. 5a-b). EBSD mapping revealed a single orientation of {112} shock-twins, and a set of planar deformation bands (PDBs) parallel to the c-axis (Fig. 5c-d). Up to 15° of cumulative misorientation across the grain was detected (Fig. 5c); the majority of cumulative misorientation across the grain is <10°, and accommodated by low-angle boundaries and PDBs.

Atlantic coast, south of the Orange River mouth (3 sites, 1502 zircon grains)

A total of 1502 detrital zircon grains were surveyed from three modern beach sand samples collected south of the Orange River mouth on the Atlantic coast. Samples 14VD79, 14VD86, and 14VD89 were collected at increasing distances of 87, 339, and 401 km, respectively, south of the Orange River mouth (Table 1) in order to detect if shocked zircon grains were being transported northward from former sites of the Orange River mouth via longshore drift. Sample 14VD89, located 401 km south of the Orange River mouth, was sampled at the mouth of the Oliphants River, which represents the southern-most location of the paleo-Orange River mouth since the Cretaceous (Dingle and Hedey, 1984). However, no shocked zircon grains were identified in the three populations surveyed, which ranged from 170 (14VD79) to 783 (14VD89) grains per sample.

Morokweng area, Northwest Province (2 sites, 153 zircon grains)

A total of 153 detrital zircon grains from two samples of modern alluvium near the Morokweng impact structure were surveyed. Sample 09VD51 was collected from the Phepane

River, and sample 09VD52 was collected from the Mashowing River; these two rivers, both dry, drain the northern and southern regions of the Morokweng structure. Both fluvial systems are tributaries of the Molopo River, which is a right-bank tributary of the Orange River; the two samples are located 1248 and 1165 km upriver from the Orange River mouth, on the southern margin of the Kalahari desert (Fig. 1). Both samples yielded few zircon grains, resulting in a relatively small number of grains surveyed. No shocked zircon grains were found in either population, which ranged from 86 (09VD51) to 67 (09VD52) grains per sample (Table 1).

U-Th-Pb geochronology

A total of 12 SHRIMP analyses were made on the three shocked zircon grains from the Orange River mouth area (Table 2). Five analyses of zircon 14VD80-373 are variably discordant and co-linear, and yield a concordia upper intercept age of 3092±18 Ma (2σ, MSWD=0.65, n=5) (Fig. 6a). Four analyses of grain 09VD48-2 are also variably discordant and co-linear, and yield a concordia upper intercept age of 3040±16 Ma (2σ, MSWD=0.63, n=4) (Fig. 6b and Table 2). Three analyses of grain 14VD77-1224 are not co-linear, but overlap in a cluster on the concordia curve, with one spot showing slight reverse discordance; together they yield a weighted mean $^{207}Pb/^{206}Pb$ age of 3130±16 Ma (2σ, MSWD=0.91, n=3) (Fig. 6c). The data from grains 09VD48-2 and 14VD80-373 show variable discordance; discordia regressions define lower intercept ages of 268±490 Ma and 809±380 Ma, respectively, which indicate that Pb-loss occurred long after the 2020 Ma Vredefort impact (Fig. 6a-b).

Discussion

Shock microstructures

The three detrital zircon grains (09VD48-2, 14VD77-1224 and 14VD80-373) discovered near the mouth of the Orange River at the Atlantic coast preserve unambiguous shock microstructures. The grains contain multiple orientations of PFs visible on external surfaces, which correlate to features visible in polished section. Each grain contains between one and three orientations of {112} twins as measured by EBSD, as well as evidence of crystal-plastic deformation accommodated by low-angle boundaries. The formation of planar microstructures and {112} shock-twins requires pressures of 20 GPa (Leroux et al., 1999; Morozova, 2015), thus confirming an unequivocal impact-provenance origin for these grains.

Provenance of the detrital shocked zircon grains

An origin from the Vredefort Dome. The microstructures described above provide clear evidence of shock deformation, but cannot alone be used to determine the provenance of the grains. The three zircon grains yield Archean ages of 3040±16, 3092±18, and 3130±16 Ma, which are interpreted as bedrock crystallization ages, given that shock-twinning has not been shown to reset U-Pb ages at the scale of a 20 μm SHRIMP spot (Cavosie et al., 2015b). The above ages correlate well with ages of bedrock exposed in the core of the Vredefort impact structure, which range from 3500 to 3010 Ma (Kamo et al., 1996; Hart et al., 1999; Moser et al., 2001; Flowers et al., 2003; Armstrong et al., 2006). Pb-loss within the analyzed zircon grains does not record the 2020 Ma Vredefort impact, and was likely caused by either the Neoproterozoic Pan-African orogeny or the 1.11 – 1.02 Ga Kibaran orogeny (Jacobs et al., 1993; Kamo et al., 1996; Reimold et al., 2000). Similar Pb-loss ages have been reported in studies of shocked zircon from Vredefort bedrock (Flowers et al., 2003; Armstrong et al., 2006; Moser et al., 2011) and in detrital shocked zircon suites in the Vaal River (Erickson et al., 2013a), which lends further support to our interpretation that the grains described here originated from the Vredefort impact structure.

The Morokweng impact structure? The possibility that the three detrital shocked zircon grains described here did not originate from the Vredefort structure was also considered. Only one other impact crater has been confirmed in the Orange River basin. The 145 Ma Morokweng impact structure, located in the Northwest Province of South Africa, is a ~70 km wide crater (Hart et al., 1997). The Morokweng structure is within the Molopo River basin, a northern right-bank tributary whose confluence with the Orange River is 635 km upriver from the Atlantic coast. The location of Morokweng inside the Orange basin allows for the possibility that detrital shocked zircon at the Orange River mouth may have originated from this structure. However an origin from Morokweng is considered unlikely for the following reasons.

The Morokweng structure is buried, and shocked bedrock is not exposed. Archean granitoids ranging from 3.0 to 2.9 Ga occur regionally but are unshocked; most local bedrock belongs to the 2.25-2.5 Ga Transvaal and Griquatown groups, which are also unshocked (Corner et al., 1997), and are too young to have yielded the ca. 3.0-3.1 Ga shocked zircon grains described here. Ephemeral streams crosscut the Morokweng structure, two of which, the Phepane and Mashowing dry rivers, were sampled for this study. Corner et al. (1997) reported shocked quartz in two of 82 cobbles sampled from the bed of the Mashowing River. However, our survey of 86 detrital zircon grains from the Mashowing River and 67 detrital zircon grains from the Phepane River did not identify any shocked zircon grains (Table 1). For the past 1000 years, a barchan dune has blocked the Molopo River 15 km upstream from its confluence with the Orange River; today the Molopo is a dry ephemeral river that only flows during infrequent floods (Bremner et al., 1990). The Morokweng impact structure likely contributed detrital shocked minerals to local fluvial systems in the Kalahari region after its formation at 145 Ma, and before subsequent burial. However, we cite the absence (or at very least, low abundance) of detrital shocked zircon in modern sediment at the site of the buried structure, the absence of exposed ca. 3.0-3.1 Ga shocked-zircon bearing bedrock, and the minimal discharge of the dry regional fluvial systems together to indicate that it is highly unlikely that detrital shocked zircon grains from the Morokweng structure are currently being transported ~1200 km downstream to the mouth of the Orange River in modern alluvium.

An unidentified impact structure? An origin of the shocked grains from an unidentified impact structure located in southern Africa was also considered, as it is possible that the grains originated from an impact crater within the Orange River basin that has yet to be identified. The Orange River basin covers nearly a million square kilometers (Bremner, 1990), and drains the western half of the Kaapvaal craton (Fig. 1). The ca. 3.0-3.1 Ga Archean crystallization ages require that the shocked zircon grains originated on the Kaapvaal craton (unless they were shocked as detrital grains in a sedimentary rock deposited pre-impact, a highly speculative scenario which we do not consider further). The three shocked zircon grains each contain {112} twins, and are thus interpreted to have originated from the central uplift of an impact structure that exposes shocked ca. 3.0-3.1 Ga Archean crust, analogous to the Vredefort Dome (e.g. Moser et al., 2011). While this explanation is speculative and not viewed as likely, the discovery of a new impact structure in southern Africa would not be unusual given the overall low density of impact craters confirmed in Africa (Spray, 2001; Reimold and Koeberl, 2014). Three new impact structures have been confirmed in Africa since 2010 (Folco et al., 2010; Ferriere et al., 2011; Chennaoui Aoudhehane et al., 2016). If a new impact structure in the Orange River basin is later discovered, the provenance characteristics of the detrital shocked grains described here can be revisited to further evaluate their potential source crater.

Taken together, the diagnostic shock microstructures, narrow range of U-Pb ages from 3040 to 3130 Ma, ubiquitous presence of shocked zircon in modern Vaal River alluvium, the definitive presence of shocked zircon in lower Orange River alluvium, the paucity of shocked zircon in modern sediment south of the Orange River mouth and near the Morokweng impact structure all support our preferred interpretation, whereby the detrital shocked zircon grains discovered on and near the Atlantic coast originated from the Vredefort impact structure, and were transported downstream by fluvial processes in the combined Vaal-Orange rivers nearly 1940 km downstream (Fig. 1).

Sedimentology of detrital shocked zircon in the Orange River

Detrital shocked zircon abundance. The abundance of detrital shocked zircon in the Vaal-Orange river system decreases with distance from their inferred point source, the Vredefort impact structure. Cavosie et al. (2010) documented detrital shocked zircon in the Vaal River within the Vredefort Dome, reporting abundances ranging from 36 – 64%. The abundance decreases downstream in the Vaal River, from 18% at 100 km to 2% at 759 km near the Vaal-Orange confluence (Erickson et al., 2013a). Results from the four samples in this study located at or near the mouth of the Orange River, summed together, yield an abundance of 0.04% (3/7326) at nearly 2000 km downriver. The abundance values cited here, based on identification of single shocked grains, are variable, and dependent on the total number of grains analyzed, which also varied among samples. While none of the samples from the Orange River mouth area yielded more than a single shocked zircon, we note the reproducibility of this result between samples 09VD48 and 14VD80, which were collected from the same location 5 years apart. These two samples were collected, processed, and analyzed by different persons, and each yielded a single shocked zircon in the population surveyed, which ranged from 1055 to 2745 grains per sample.

Paucity of shocked zircon in the middle Orange River. One puzzling result of this study is that no detrital shocked zircon grains were found in samples from the middle Orange River. The middle Orange River sample suite includes five modern alluvium samples located from 761 to 1219 km downstream from the Vredefort Dome, including sample 14VD69, located only 2 km below the Vaal-Orange confluence. The number of grains investigated per sample from the middle Orange River (samples 09VD38, 09VD44, 09VD45, and 09VD46) is somewhat lower (<500 grains per sample) in comparison with the number of grains investigated in samples near the Orange River mouth (352-3174 grains per sample). However, >1000 grains were surveyed from the sample 2 km below the Vaal-Orange confluence that did not yield any shocked grains (14VD69, 0/1153). This sample is located only ~5 km further downstream from a known detrital shocked zircon site in the Vaal River (sample 09VD41) that yielded 5 shocked grains from a population of 253 grains investigated (2%, Erickson et al., 2013a). We predicted identifying up to 20 detrital shocked zircon grains in the population of 1153 grains surveyed from sample 14VD69 based on the prior results from sample 09VD41. One possible explanation for not finding shocked zircon in the middle Orange River is that the high sediment production and high runoff from the upper Orange may dramatically dilute sediment input from the Vaal River near and below the confluence.

Mode of detrital transport. The mode of transport that resulted in detrital zircon from the Vredefort Dome being present nearly 2000 km downriver merits further discussion. Each of the three detrital shocked grains described here were collected as modern sediment (beach sand and alluvium) in environments uniquely dominated by medium-to-coarse grained sand, with no obvious coarser material locally present (e.g., pebbles or larger particles). Based on field observations, the zircon grains appear to have been transported to and deposited at the sites where they were collected as loose grains. However, the three shocked zircon grains have remarkably well preserved prisms and pyramids, and show only minor evidence of abrasion and rounding. In this regard, their exterior surfaces are similar to those of detrital shocked zircon grains described from the Vaal River, where the planar microstructures are pervasively etched, but the grains otherwise show little evidence of sedimentary abrasion (Cavosie et al., 2010; Erickson et al., 2013a). While we cannot rule out the possibility that these grains were incorporated in larger particles of rock for part of their transport history in the Vaal-Orange rivers, we have no evidence to support this mode of transport, as clasts of Vredefort-derived bedrock have thus far not been reported downriver of the impact structure. The absence of pronounced sedimentary abrasion (and subsequent rounding) in grains that have experienced distal transport in fluvial systems might instead reflect the lack of an eolian transport history. Detailed studies of texturally mature Precambrian quartz arenite occurrences have identified the critical role of eolian transport in both the abrasion and rounding of detrital quartz grains and associated accessory minerals (e.g., Dott, 2003). Given that the Vaal River cross-cuts and is entrenched in shocked bedrock at the Vredefort Dome, it is reasonable to conclude that shocked zircon grains transported in the Vaal-Orange rivers experienced little, if any, history of eolian transport. We thus attribute the well-preserved forms of the shocked zircon grains on and near the Atlantic coast to the dominance of fluvial processes as the main mechanism that transported the grains in modern alluvium nearly 2000 km downriver from the Vredefort structure.

Our results from southern Africa, together with previous studies, suggest that SEM imaging surveys for detrital shocked minerals in alluvium eroded from known impact structures should be able to identify shocked grains in a sample as small as ~250 zircon grains if they are located <750 km from the source crater (Cavosie et al., 2010; Erickson et al., 2013a). However, the surveyed population should be expanded to >1000 zircon grains when searching for distally transported detrital shocked grains (>750 km), or if the location of the source crater is unknown or only suspected (Reddy et al., 2015). In our experience, surveying populations of 1000 (or more) grains per sample by SEM is practical from an analytical point of view, and more significantly, allows an evaluation of the presence of shocked zircon at a minimum abundance level of 0.1% (1/1000). The size of the impact structure, level of erosion, extent of exposed shocked bedrock, and abundance of zircon-bearing target rock will all influence the sedimentary record of detrital shocked zircon. Additional studies are required at other sites to evaluate if the erosional record of the Vredefort impact structure is a general result, or a consequence of the unique geologic history of the region (c.f, Thomson et al., 2014).

Implications

These results demonstrate that shocked zircon from ancient and deeply eroded impact structures can survive fluvial transport to distal localities, and preserve impact evidence in the form of diagnostic shock microstructures. Our results greatly expand known transport distances for detrital shocked zircon previously documented within the Vredefort Dome and the Vaal River (Cavosie et al., 2010; Erickson et al., 2013a).

One implication of the discovery of detrital shocked zircon on the Atlantic coast of southern Africa is that shocked grains are evidently resilient enough to survive distal fluvial transport, and can end up in areas beyond the drainage basin they originated in. Sediment, including detrital zircon grains, from the Orange River basin has been found along the Atlantic coast of Namibia (Stone, 2013), as far as 700 km north of the Orange River mouth, at Walvis Bay (Lancaster and Ollier, 1983; Bluck et al., 2007; Vermeesch et al., 2010). The above observations clearly imply that Vredefort-derived shocked zircon grains are likely to occur in detrital populations at these locations along the coast of Namibia, albeit at predictably low abundance levels (<0.1%).

Considering the process of distal transport of shocked grains further back in time, detrital shocked zircon grains from Phanerozoic and Precambrian impact structures are predicted to reside in younger sedimentary rocks. Detrital grains as old as 4.4 Ga (Cavosie et al., 2005; Cavosie et al., 2007; Valley et al., 2014) provide clear evidence that populations of ancient detrital zircon are preserved, which may contain shocked grains at detectable abundance levels (e.g., <0.1%). Discovery of such grains would provide the first ground-truth evidence for the earliest meteorite bombardment history of Earth, and allow the testing of models for establishment of habitable conditions on the early Earth.

Acknowledgments

We thank John Fournelle, Brian Hess, Stephen Hughes, Clark Johnson, Desmond Moser, Maya Pincus, Steve Reddy, Michael Spicuzza, Nick Timms, John Valley, and Joseph Wooden for assistance and access to laboratories. Editor Sandra Piazolo, Roger Gibson, and Urs Klötzli provided valuable review comments. This work was supported NSF (EAR-0838300, EAR-1145118), the NASA Astrobiology program, the SHRIMP and Microscopy and Microanalysis Facilities at Curtin University, and a Curtin Research Fellowship.

References cited

Armstrong, R.A., Lana, C., Reimold, W.U., and Gibson, R.L. (2006) SHRIMP zircon age constraints on Mesoarchean crustal development in the Vredefort dome, central Kaapvaal Craton, South Africa. Geological Society of America Special Paper 405, 233-253.

Barth, A.P., and Wooden, J.L. (2010) Coupled elemental and isotopic analyses of polygenetic zircons from granitic rocks by ion microprobe, with implications for melt evolution and the sources of granitic magmas. Chemical Geology, 277, 149-159.

Benade, C. (1988) Episodic flood events in the Orange River system – an ecological perspective. Paper 3.6 in Proceedings of the conference on floods in perspective, p. 1-16. Department of Water Affairs and Forestry, Pretoria.

Black, L.P., Kamo, S.L., Allen, C.M., Davis, D.W., Aleinikoff, J.N., Valley, J.W., Mundil, R., Campbell, I.H., Korsch, R.J., Williams, I.S. and Foudoulis, C. (2004) Improved $^{206}Pb/^{238}U$ microprobe geochronology by the monitoring of a trace-element-related matrix effect; SHRIMP, ID-TIMS, ELA-ICP-MS and oxygen isotope documentation for a series of zircon standards. Chemical Geology, 205, 115-140.

Bluck, B.J., Ward, J.D., Cartwright, J., Swart, R. (2007) The Orange River, southern Africa: an example of a wave-dominated sediment dispersal system in the South Atlantic Ocean. Journal of the Geological Society 164, 341-351.

Bohor, B.F., Betterton, W.J., and Krogh, T.E. (1993) Impact-shocked zircons: discovery of shock-induced textures reflecting increasing degrees of shock metamorphism. Earth and Planetary Science Letters, 119, 413-424.

Bremner, J.M., Rogers, J., and Willis, J.P. (1990) Sedimentological aspects of the 1988 Orange River floods. Transactions of the Royal Society of South Africa, 47, 247-294.

Cavosie, A.J., Valley, J.W., Wilde, S.A., and EIMF (2005) Magmatic $\delta^{18}O$ in 4400–3900 Madetrital zircons: a record of the alteration and recycling of crust in the Early Archean. Earth and Planetary Science Letters, 235, 663–681.

Cavosie, A.J., Valley, J.W., Wilde, S.A. (2007) The oldest terrestrial mineral record: A review of 4400 to 3900 Ma detrital zircons from Jack Hills, Western Australia. In, M.J. van Kranendonk, R.H. Smithies, and V.C. Bennett, Eds., World's Oldest Rocks, p. 91-111. Elsevier Science, Amsterdam.

Cavosie, A.J., Quintero, R.R., Radovan, H.A., and Moser, D.E. (2010) A record of ancient cataclysm in modern sand: Shock microstructures in detrital minerals from the Vaal River, Vredefort Dome, South Africa. Geological Society of America Bulletin, 122, 1968-1980.

Cavosie, A.J., Erickson, T.M., and Timms, N.E. (2015a) Nanoscale record of ancient shock deformation: reidite ($ZrSiO_4$) in sandstone at the Ordovician Rock Elm impact crater. Geology, 43, 315-318.

Cavosie, A.C., Erickson, T.M., Timms, N.E., Reddy, S.M., Talavera, C., Montalvo, S.D., Pincus, M.R., Gibbon, R.J., and Moser, D. (2015b) A terrestrial perspective on using ex situ shocked zircons to date lunar impact. Geology, 43, 999-1002.

Cavosie, A.J., Timms, N.E., Erickson, T.M., Hagerty, J.J., and Hörz, F.P. (2016) Transformations to granular zircon revealed: Twinning, reidite, and ZrO_2 in shocked zircon from Meteor Crater (Arizona, USA). Geology, 44, 703-706.

Chennaoui Aoudhehane, H., El Kerni, H., Reimold, W., Baratoux, D., Koeberl, C., Bouley, S., and Aoudjehane, M. (2016) The Agoudal (High Atlas Mountains, Morocco) shatter cone conundrum: A recent meteorite fall onto the remnant of an impact site. Meteoritics & Planetary Science, 51, 1497-1518.

Compton, J.S., and Maake, L. (2007) Source of the suspended load of the upper Orange River, South Africa. South Africa Journal of Geology, 110, 339-348.

Corner, B., Reimold, W.U., Brandt, D., and Koeberl, C. (1997) Morokweng impact structure, Northwest Province, South Africa: geophysical imaging and shock petrographic studies. Earth and Planetary Science Letters, 146, 351-364.

de Wit, M.C.J., Marshall, T.R., and Partridge, T.C. (2000) Fluvial Deposits and Drainage Evolution. In T.C. Partridge and R.R. Maud, Eds., The Cenozoic of Southern Africa, p. 55-72. Oxford University Press, Oxford.

Dott, R.H. Jr. (2003) The importance of eolian abrasion in supermature quartz sandstones and the paradox of weathering on vegetation-free landscapes. Journal of Geology, 111, 387-405.

Erickson, T.M., Cavosie, A.J., Moser, D.E., Barker, I.R., Radovan, H.A., and Wooden, J. (2013a) Identification and provenance determination of distally transported, Vredefort-derived shocked minerals in the Vaal River, South Africa using SEM and SHRIMP-RG techniques. Geochimica et Cosmochimica Acta, 107, 170-188.

Erickson, T.M., Cavosie, A.J., Moser, D.E., Barker, I.R., and Radovan, H.A. (2013b) Correlating planar microstructures in shocked zircon from the Vredefort Dome at multiple scales: Crystallographic modeling, external and internal imaging, and EBSD structural analysis. American Mineralogist, 98, 53-65.

Erickson, T.M., Cavosie, A.J., Pearce, M.A., Timms, N.E., and Reddy, S.M. (2016) Empirical constraints on shock features in monazite using shocked zircon inclusions. Geology, 44, 635-638.

Ferrier, L., Lubala, F.R.T., Osinski, G.R., and Kaseti, P.K. (2011) The newly confirmed Luizi impact structure, Democratic Republic of Congo – Insights into central uplift formation and post-impact erosion. Geology, 39, 851-854.

Flowers, R.M., Moser, D.E., and Hart, R.J. (2003) Evolution of the amphibolite-granulite facies transition exposed by the Vredefort impact structure, Kaapvaal craton, South Africa. The Journal of Geology, 111, 455-470.

Folco, L., Di Martino, M., Barkooky, A.E.,D'Orazio, M.,Lethy, A., Urbini, S., Nicolosi, L., Hafez, M., Cordier, C., van Ginneken, M., and others. (2010) The Kamil Crater in Egypt. Science, 329, no. 5993, 804.

French, B.M. (1998) Traces of Catastrophe: A Handbook of Shock-Metamorphic Effects in Terrestrial Meteorite Impact Structures, 120 p. Lunar and Planetary Institute, Houston.

Garzanti, E., Ando, S., Vezzoli, G., Lustrino, M., Boni, M., and Vermeesch, P. (2012) Petrology of the Namib Sand Sea: Long-distance transport and compositional variability in the wind-displaced Orange Delta. Earth-Science Reviews, 112, 173-189.

Gibbon, R.J., Granger, D.E., Kuman, K., and Patridge, T.C. (2009) Early Acheulean technology in the Rietputs Formation, South Africa, dated with cosmogenic nuclides. Journal of Human Evolution, 56, 152-160.

Gibson, R.L. and Reimold, W.U. (2008) Geology of the Vredefort Impact Structure: A Guide to Sites of Interest, 181 p. Council for Geoscience, Pretoria.

Gibson, R.L., Armstrong, R.A., and Reimold, W.U. (1997) The age and thermal evolution of the Vredefort impact structure: A single-grain U-Pb zircon study. Geochimica Acta, 61, 1531-1540.

Gibson, R.L., Reimold, W.U., and Stevens, G. (1998) Thermal-metamorphic signature of an impact event in the Vredefort dome, South Africa. Geology, 26(9), 787-790.

Glass, B.P., and Liu, S. (2001) Discovery of high-pressure ZrSiO4 polymorph in naturally occurring shock-metamorphosed zircons. Geology, 29, 371-373.

Grieve, R. and Therriault, A. (2000) Vredefort, Sudbury, Chicxulub: Three of a Kind? Annual Reviews in Earth and Planetary Science, 28, 305–38.

Hart, R.J., Andreoli, M.A.G., Tredoux, M., Moser, D., Ashwal, L.D., Eide, E.A., Webb, S.J., and Brandt, D. (1997) Late Jurassic age for the Morokweng impact structure, southern Africa. Earth and Planetary Science Letters, 147, 25-35.

Hart, R., Moser, D., and Andreoli, M. (1999) Archean age for the granulite facies metamorphism near the center of the Vredefort structure, South Africa. Geology, 27, 1091-1094.

Jacobs, J., Thomas, R.J., and Weber, K. (1993) Accretion and indentation tectonics at the southern edge of the Kaapvaal craton during the Kibaran (Grenville) orogeny. Geology, 21, 203-206.

Kamo, S.L., Reimold, W.U., Krogh, T.E., and Colliston, W.P. (1996) A 2.023 Ga age for the Vredefort impact event and a first report of shocked metamorphosed zircon in pseudotachylytic breccias and granophyres. Earth and Planetary Science Letters, 144, 369-387.

Lancaster, N., and Ollier, C.D. (1983) Sources of sand for the Namib sand sea. Zeitschrift fur Geomorphology Supplement Band, 45, 71-83.

Leroux, H., Reimold, W.U., Koeberl, C., Hornemann, U., and Doukhan, J.C. (1999) Experimental shock deformation in zircon: a transmission electron microscopic study. Earth and Planetary Science letters, 169, 291-301.

Losiak, A., Kohout, K., Sullivan, K.O., Thaisen, K., and Weider, S. (2008) Lunar Impact Crater Database [Online]. Available: http://www.lpi.usra.edu/resources/ [accessed May 14, 2016]. Lunar and Planetary Institute, Universities Space Research Association, Houston, Texas.

Ludwig, K.R. (2001a) SQUID 1.02, A User's Manual: Berkeley Geochronological Center Special Publication No. 2.

--- (2001b) User's Manual for Isoplot/Ex rev. 2.49: A Geochronological Toolkit for Microsoft Excel: Berkeley Geochronological Center Special Publication No. 1a.

Melosh, H.J. (1989) Impact Cratering: A Geologic Process, 245 p. Oxford University Press, New York.

Morozova, I. (2015) Strength study of zircon under high pressure, 112 p. PhD. thesis, University of Western Ontario, London.

Moser, D.E. (1997) Dating the shock wave and thermal imprint of the giant Vredefort impact, South Africa. Geology, 25, 7-10.

Moser, D.E., Flowers. R.M., and Hart, R.J. (2001) Birth of the Kaapvaal tectosphere 3.08 billion years ago. Science, 291, 465-468.

Moser, D.E., Cupelli, C.L., Barker, I.R., Flowers, R.M., Bowman, J.R., Wooden, J., and Hart, J.R. (2011) New zircon shock phenomena and their use for dating and reconstruction of large impact structures revealed by electron nanobeam (EBSD, CL, EDS) and isotopic U-Pb and (U-Th)/He analysis of the Vredefort dome. Canadian Journal of Earth Sciences, 48, 117-139.

Nasdala, L., Hofmeister, W., Norberg, N., Mattinson, J.M., Corfu, F., Dörr, W., Kamo, S.L., Kennedy, A.K., Kronz, A., Reiners, P.W., and others. (2008) Zircon M257- a homogeneous natural reference material for the ion microprobe U-Pb analysis of zircon. Geostandards and Geoanalytical Research, 32, 247-265.

Reddy, S.M., Timms, N.E., Pantleon, W., and Trimbly, P. (2007) Quantitative characterization of plastic deformation of zircon and geological implications. Contributions to Mineralogy and Petrology, 153, 625-645.

Reddy, S.M., Johnson, T.E., Fischer, S., Rickard, W.D.A., and Taylor, R.J.M. (2015) Precambrian reidite discovered in shocked zircon from the Stac Fada impactite, Scotland. Geology, 43, 899-902.

Reimold, W.U., and Koeberl, C. (2014) Impact structures in Africa: A review. Journal of African Earth Sciences, 93, 57-175.

Reimold, W.U., Pybus, G.Q.Y., Kruger, F.J., Layer, P.W., and Koeberl, C. (2000) The Anna's Rust Sheet and related gabbroic intrusions in the Vredefort Dome-Kibaran magmatic event on the Kaapvaal Craton and beyond? Journal of African Earth Sciences, 31, 314, 499-521.

Spray, J. (2001) Earth Impact Database [Online]. Available: www.passc.net/EarthImpactDatabase/index.html [accessed August 23, 2016]. Planetary and Space Science Center, University of New Brunswick, Fredericton, New Brunswick, Canada.

Stone, A.E.C. (2013) Age and dynamics of the Namib Sand Sea: A review of chronological evidence and possible landscape development models. Journal of African Earth Sciences, 82, 70-87

Therriault, A.M., Grieve, R.A.F., and Reimold, W.U. (1997) Original size of the Vredefort structure: Implications for the geological evolution of the Witwatersrand Basin. Meteoritics and Planetary Science, 32, 71-77.

Thomson, O.A., Cavosie, A.J., Moser D.E., Barker, I., Radovan, H.A., and French, B.M. (2014) Preservation of detrital shocked minerals derived from the 1.85 Ga Sudbury impact structure in modern alluvium and Holocene glacial deposits. Geological Society of America Bulletin, 126, 720-737.

Timms, N.E., Reddy, S.M., Healy, D., Nemchin, A.A., Grange, M.L., Pidgeon, R.T., and Hart, R. (2012) Resolution of impact-related microstructures in lunar zircon: A shock-deformation mechanism map. Meteoritics and Planetary Science, 47, 120-141.

Valley, J.W., Cavosie, A.J., Ushikubo, T., Reinhard, D.A., Lawrence, D.F., Larson, D.J., Clifton, P.H., Kelly, T.F., Wilde, S.A., Moser, D.E., and Spicuzza, M.J. (2014) Hadean age for a post-magma-ocean zircon confirmed by atom-probe tomography. Nature Geoscience, 7, 219-223.

Vermeesch, P., Fenton, C.R., Kober, F., Wiggs, G.F.S., Bristow, C.S., and Xu, S. (2010) Sand residence times of one million years in the Namib Sand Sea from cosmogenic nuclides. Nature Geoscience 3, 862-865.

Wieland, F., Gibson, R.L., and Reimold, W.U. (2005) Structural analysis of the collar of the Vredefort Dome, South Africa – Significance for impact- related deformation and central uplift formation. Meteoritics and Planetary Science, 40, 1537-1554.

Wittmann, A., Kenkmann, T., Schmitt, R.T., and Stöffler, D. (2006) Shock-metamorphosed zircon in terrestrial impact craters. Meteoritics and Planetary Science, 41, 433-454.

Figure Captions

Figure 1. Simplified map of southern Africa. (**a**) Significant elements include the Kaapvaal craton, Vredefort Dome, Vaal and Orange river basins (shaded), and the subdivisions of the

Orange River. Stars show locations of sediment samples. (**b**) Sample locations near and at the Orange River mouth on the Atlantic coast.

Figure 2. Exterior images of three detrital shocked zircon grains using backscattered electrons. (**a**) Image of zircon 14VD77-1224, found in an Orange River sandbar 15 km upriver from the Atlantic coast. (**b**) Close-up image showing 2 sets of PFs. (**c**) Close-up image showing 3 sets of PFs. (**d**) Image of zircon 14VD80-373, found in beach sand on the Atlantic coast. (**e**) Close-up image showing 4 sets of PFs (**f**) Close-up image showing 3 sets of PFs. (**g**) Image of zircon 09VD48-2, found in beach sand on the Atlantic coast. (**h**) Close-up image showing 1 set of PFs. (**i**) Close-up image showing 2 sets of PFs. Arrows indicate orientations of planar fractures.

Figure 3. Interior images of grain 14VD77-1224. (**a**) BSE image showing three PF orientations (arrows). (**b**) CL image showing oscillatory zoning and location of geochronology analyses with $^{207}Pb/^{206}Pb$ ages (in Ma). (**c**) Combined band contrast (BC), grain boundary (GB) and texture component (TC) map showing twins (red lines) and crystal-plastic deformation. Red cross indicates reference location. (**d**) Orientation map showing three sets of twins, labeled (t1-t3). This map combines BC, GB, and is colored with an inverse pole figure (IPF-Z) scheme. (**e**) Stereonets (lower hemisphere) of orientation data from (**d)** showing crystallographic relationship between twins and host zircon. The twins are sets of lamellae orientated 65º about {110}; each twins shares a {112} axis with the host grain.

Figure 4. Images of grain 14VD80-373. (**a**) BSE image showing one PF set (arrow). (**b**) CL image showing disturbed zoning and location of geochronology analyses with $^{207}Pb/^{206}Pb$ ages (in Ma). (**c**) Combined band contrast (BC), grain boundary (GB) and texture component (TC) map showing twins (red lines) and crystal-plastic deformation. Red cross indicates reference location. (**d**) Orientation map showing one sets of twins (labeled t1). This map combines BC,

GB, and is colored with an inverse pole figure (IPF-Z) scheme. (**e**) Stereonets (lower hemisphere) of orientation data from (**d)** showing crystallographic relationship between twins and host zircon.

Figure 5. Interior images of grain 09VD48-2. (**a**) BSE image showing two PF sets (arrows). (**b**) CL image showing sector zoning and location of geochronology analyses with $^{207}Pb/^{206}Pb$ ages (in Ma). (**c**) Orientation map showing one set of twins (red lines), planar deformation bands (PDB), and crystal-plastic deformation. Red cross indicates reference location. (**d**) Stereonets (lower hemisphere) of orientation data from **(c)** showing crystallographic relationship between twins and host zircon.

Figure 6. U-Pb concordia diagrams. Results of the SHRIMP analyses on zircon grains (**a**) 14VD80-373, (**b**) 09VD48-2, and (**c**) 14VD77-1224. Regressions in the top two panels are not anchored to the concordia curve.

Table 1. Sample location information and summary of shocked zircon search.

Sample	Latitude	Longitude	Zrn[a], grains surveyed	Zrn, shocked	Zrn, % shocked	Distance (km)
Middle Orange River[b]						
14VD69	S29°04.626'	E23°37.358'	1153	0	0	761
09VD38	S29°13.087'	E23°21.045'	481	0	0	776
09VD44	S28°52.803'	E21°59.145'	379	0	0	1054
09VD45	S28°43.740'	E20°59.142'	41	0	0	1202
09VD46	S28°38.121'	E21°05.377'	133	0	0	1219
		subtotal	2187			
Atlantic coast and Lower Orange River, near Orange River mouth[b]						
14VD77	S28°33.344'	E16°32.903'	3174	1	0.03	1925
14VD76	S28°34.015'	E16°30.439'	352	0	0	1929
14VD80[c]	S28°38.59'	E16°28.32'	2745	1	0.04	1939
09VD48[c]	S28°38.59'	E16°28.32'	1055	1	0.09	1939
		subtotal	7326			
Atlantic coast, south of Orange River mouth[d]						
14VD79	S29°15.180'	E16°52.055'	170	0	0	87
14VD86	S31°15.357'	E17°51.726'	549	0	0	339
14VD89	S31°42.321'	E18°11.559'	783	0	0	401
		subtotal	1502			
Near the Morokweng impact structure[d]						
09VD52	S26°35.153'	E22°40.559'	67	0	0	1165
09VD51	S25°47.282'	E22°54.882'	86	0	0	1248
		subtotal	153			
Total			11168	3	0.03	

[a] Zrn = zircon.

[b] Distance cited is from the Route 53 bridge in Parys to the sample location.

[c] Collected from a 2 km long sand spit at the Orange River mouth on the Atlantic coast; the location cited is in the middle of the sand spit.

[d] Distance cited is from the sample location to the mouth of the Orange River.

Table 2. Detrital shocked zircon U-Th-Pb isotopic data from SHRIMP.

Spot	U (ppm)	Th (ppm)	Th/U	% comm $^{206}Pb^{a}$	$^{204}Pb/^{206}Pb$	$^{208}Pb^{a}/^{232}Th$	$^{207}Pb^{a}/^{235}U$	$^{206}Pb^{a}/^{238}U$	$^{207}Pb^{a}/^{206}Pb^{a}$	$^{206}Pb^{a}/^{238}U$ Age (Ma)	$^{207}Pb^{a}/^{206}Pb^{a}$ Age (Ma)	% conc
14VD77-1224												
1224-1	96	88	0.94	0.18	0.0001	0.139 ± 0.003	20.32 ± 0.3912	0.6055 ± 0.0106	0.24341 ± 0.00198	3052 ± 85	3142 ± 26	97
1224-2	348	468	1.39	0.17	0.0001	0.153 ± 0.002	19.92 ± 0.2911	0.6000 ± 0.0074	0.24077 ± 0.00187	3030 ± 60	3125 ± 25	97
1224-3	207	234	1.17	0.17	0.0001	0.161 ± 0.003	20.99 ± 0.3964	0.6367 ± 0.0095	0.23912 ± 0.00278	3176 ± 75	3114 ± 37	102
14VD80-373												
373-1	183	61	0.35	1.03	0.00057	0.126 ± 0.003	16.74 ± 0.2413	0.5303 ± 0.0070	0.22893 ± 0.00133	2743 ± 59	3045 ± 19	90
373-2	107	46	0.45	0.80	0.00044	0.126 ± 0.005	17.64 ± 0.2903	0.5563 ± 0.0083	0.22994 ± 0.00156	2851 ± 69	3052 ± 22	93
373-3	340	175	0.53	0.39	0.00021	0.159 ± 0.003	19.06 ± 0.2787	0.5893 ± 0.0084	0.23463 ± 0.00081	2987 ± 68	3084 ± 11	97
373-4	263	112	0.44	0.26	0.00014	0.148 ± 0.005	18.85 ± 0.2405	0.5875 ± 0.0072	0.23265 ± 0.00087	2979 ± 58	3070 ± 12	97
373-5	283	94	0.35	0.43	0.00024	0.149 ± 0.002	18.46 ± 0.2378	0.5753 ± 0.0070	0.23269 ± 0.00095	2930 ± 58	3071 ± 13	95
09VD48-2												
48-1	130	150	1.19	0.04	0.00002	0.5379 ± 0.0110	16.767 ± 0.356	0.5379 ± 0.0110	0.22608 ± 0.00122	2775 ± 92	3024 ± 17	92
48-2	85	56	0.68	0.27	0.00015	0.5935 ± 0.0127	18.595 ± 0.414	0.5935 ± 0.0127	0.22724 ± 0.00143	3004 ± 102	3033 ± 20	99
48-3	101	91	0.93	0.59	0.00033	0.5656 ± 0.0119	17.885 ± 0.423	0.5656 ± 0.0119	0.22933 ± 0.00250	2890 ± 98	3047 ± 35	95
48-4	112	94	0.87	0.02	0.00001	0.5693 ± 0.0119	17.910 ± 0.384	0.5693 ± 0.0119	0.22815 ± 0.00110	2905 ± 98	3039 ± 15	96

comm = common; conc = concordance.

[a] Indicates a ^{204}Pb corrected Pb value after Ludwig, 2001a.

Uncertainty in isotopic ratios and ages are listed at 2σ.

The % concordance is calculated as follows: [($^{206}Pb^{a}/^{238}U$ age)/($^{207}Pb^{a}/^{206}Pb^{a}$ age)] x 100%.

This is a preprint, the final version is subject to change, of the American Mineralogist (MSA)
Cite as Authors (Year) Title. American Mineralogist, in press.
(DOI will not work until issue is live.) DOI: http://dx.doi.org/10.2138/am-2017-5857CCBYNCND

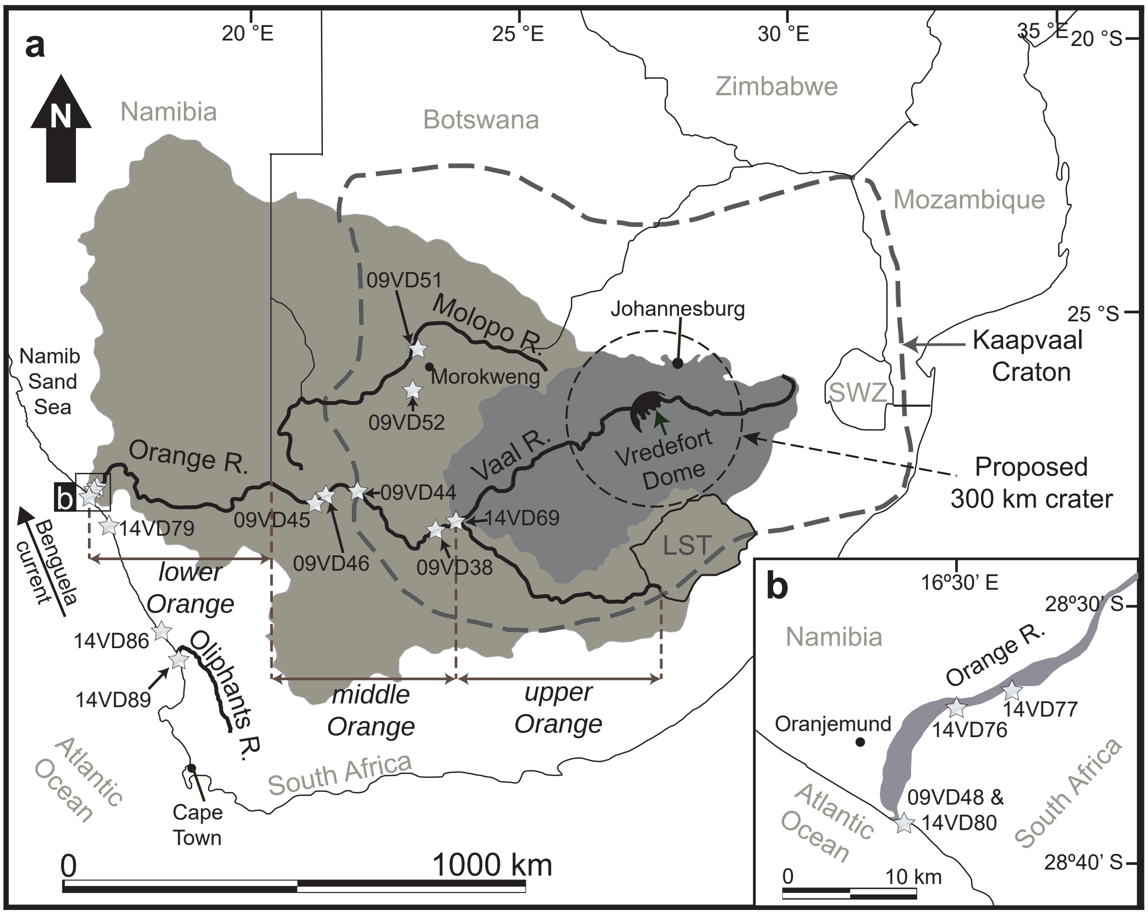

Figure 1

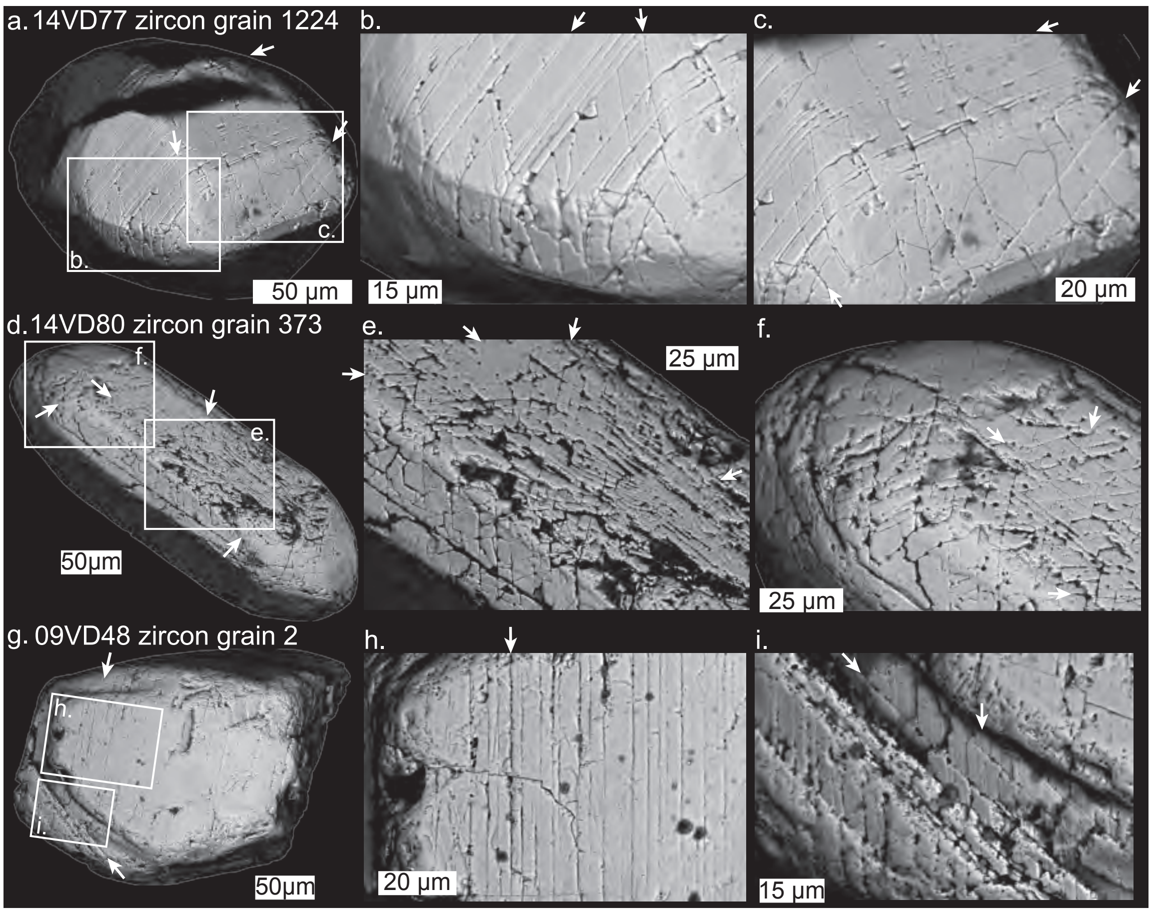
a. 14VD77 zircon grain 1224
b.
c.
50 µm
15 µm
20 µm
d. 14VD80 zircon grain 373
e.
f.
50µm
25 µm
25 µm
g. 09VD48 zircon grain 2
h.
i.
50µm
20 µm
15 µm

Figure 2

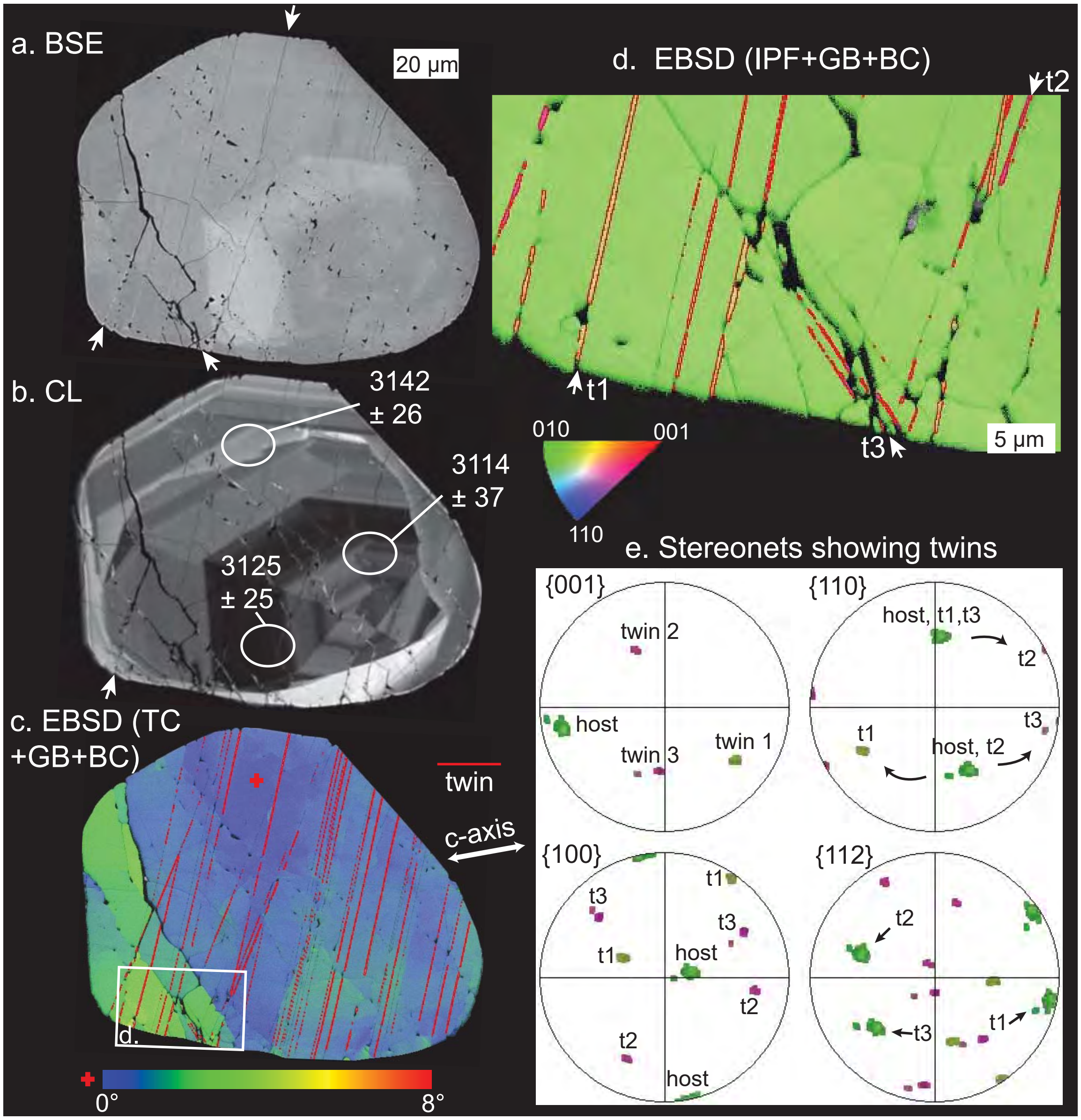
a. BSE
20 µm
b. CL
3142
± 26
3114
± 37
3125
± 25
c. EBSD (TC
+GB+BC)
twin
c-axis
d.
0°
8°
d. EBSD (IPF+GB+BC)
t2
t1
t3
5 µm
010
001
110
e. Stereonets showing twins
{001}
twin 2
host
twin 1
twin 3
{110}
host, t1,t3
t2
t3
t1
host, t2
{100}
t1
t3
t3
t1
host
t2
t2
host
{112}
t2
t3
t1

Figure 3

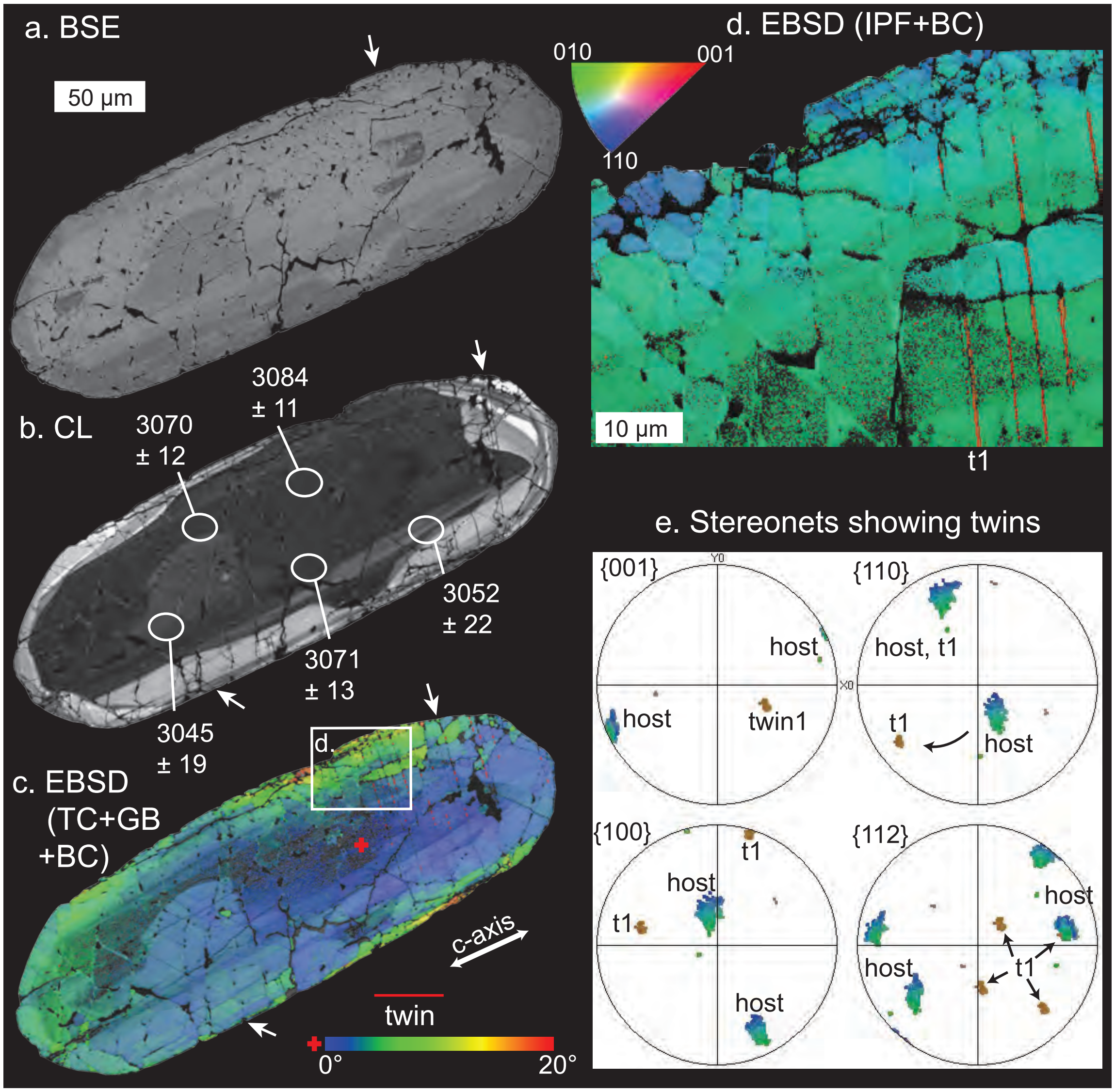
a. BSE
50 μm
b. CL
3070 ± 12
3084 ± 11
3052 ± 22
3071 ± 13
3045 ± 19
c. EBSD (TC+GB +BC)
d.
c-axis
twin
0°
20°
d. EBSD (IPF+BC)
010
001
110
10 μm
t1
e. Stereonets showing twins
{001}
host
host
twin1
{110}
host, t1
t1
host
{100}
t1
host
t1
host
{112}
host
host
t1

Figure 4

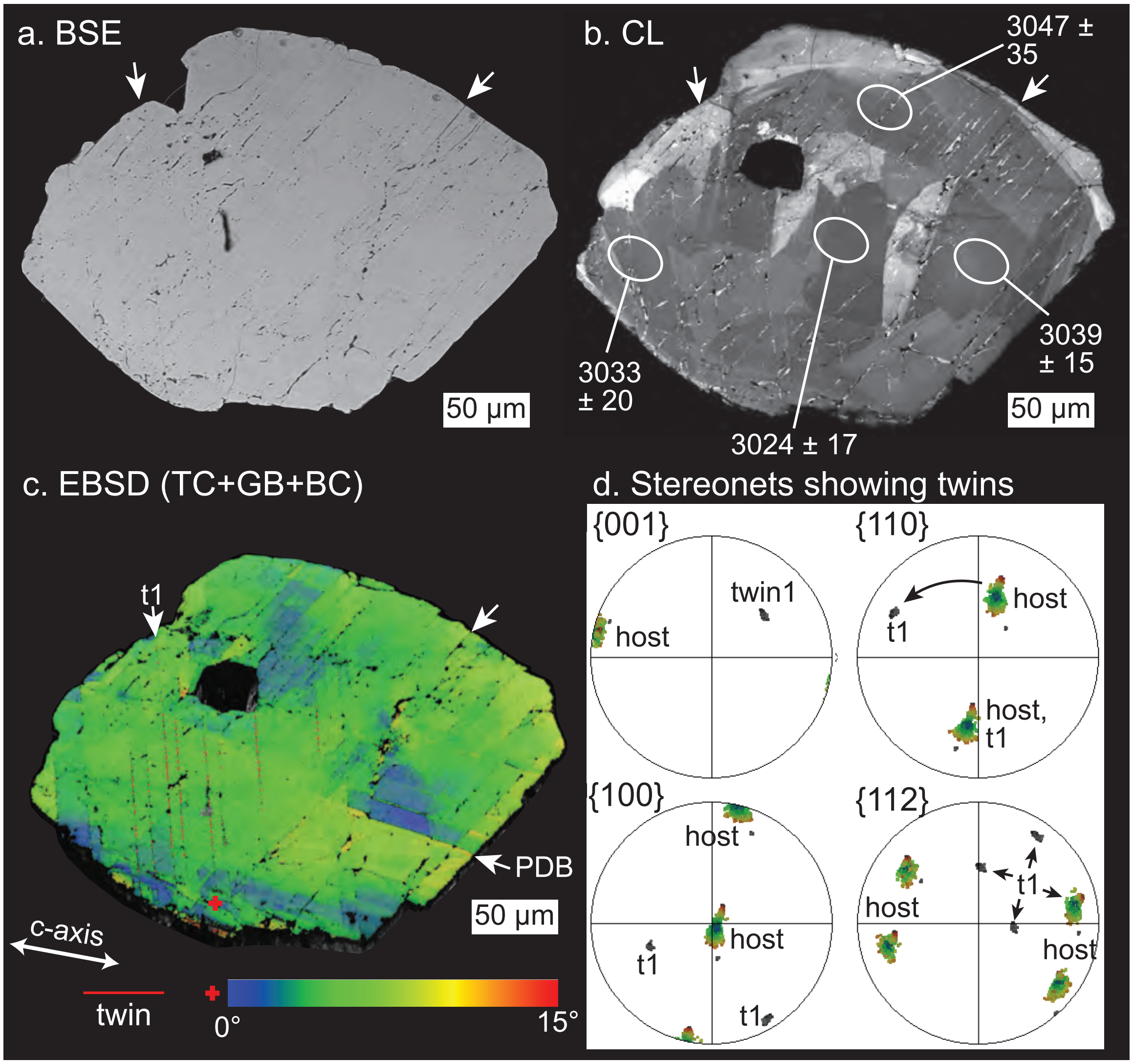
a. BSE
50 µm
b. CL
3047 ± 35
3033 ± 20
3024 ± 17
3039 ± 15
50 µm
c. EBSD (TC+GB+BC)
t1
PDB
50 µm
c-axis
twin
0°
15°
d. Stereonets showing twins
{001}
twin1
host
{110}
host
t1
host, t1
{100}
host
host
t1
t1
{112}
t1
host
host

Figure 5

This is a preprint, the final version is subject to change, of the American Mineralogist (MSA)
Cite as Authors (Year) Title. American Mineralogist, in press.
(DOI will not work until issue is live.) DOI: http://dx.doi.org/10.2138/am-2017-5857CCBYNCND

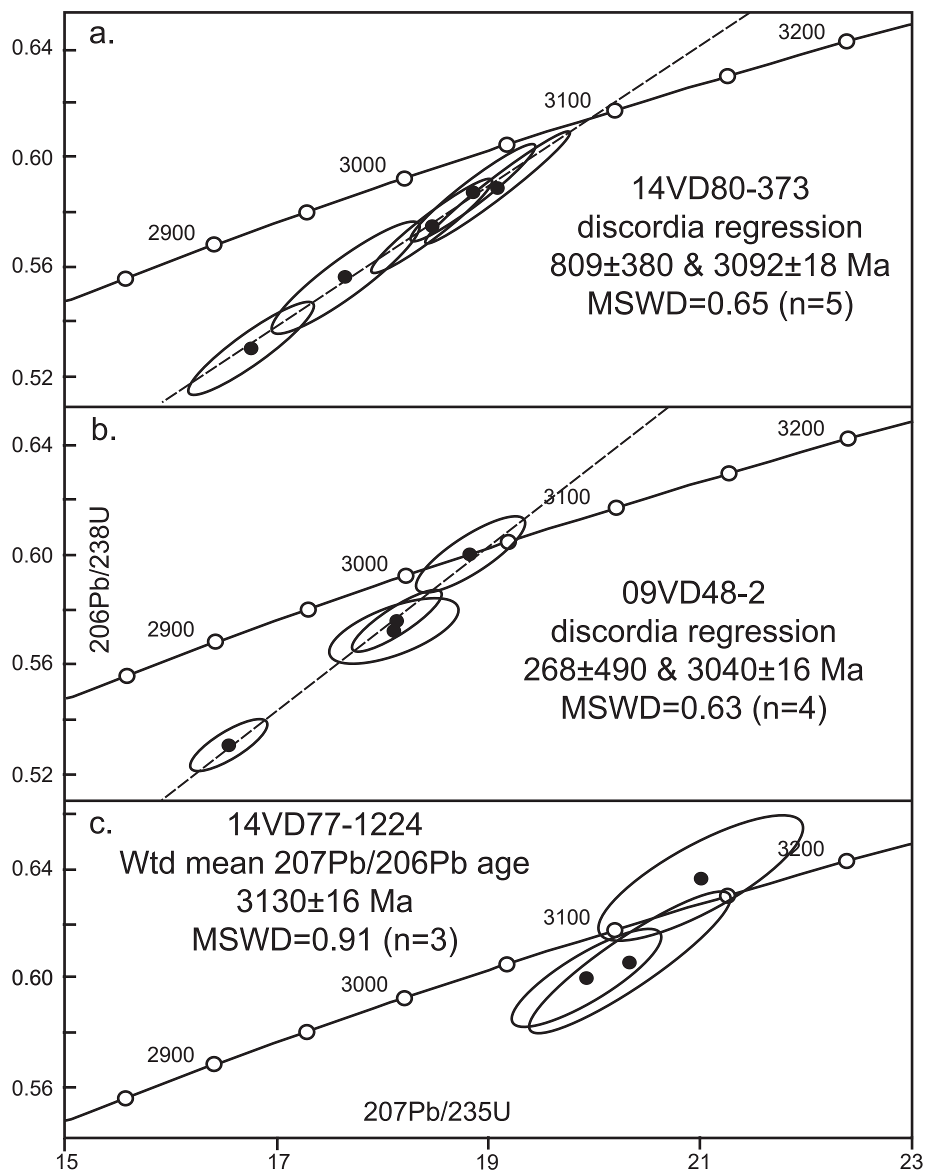

Figure 6